UC-403

LBL-26121

Lawrence Berkeley Laboratory

UNIVERSITY OF CALIFORNIA

EARTH SCIENCES DIVISION

RECEIVED
LAWRENCE
BERKELEY LABORATORY

DEC 21 1988

LIBRARY AND
DOCUMENTS SECTION

To be presented at the Tenth SPE Symposium on
Reservoir Simulation, Houston, TX,
February 6–8, 1989

A New Semi-Analytical Method for Numerical Simulation of Fluid and Heat Flow in Fractured Reservoirs

K. Pruess and Y.S. Wu

October 1988

For Reference

Not to be taken from this room

LBL-26121

Prepared for the U.S. Department of Energy under Contract Number DE-AC03-76SF00098.

DISCLAIMER

This document was prepared as an account of work sponsored by the United States Government. While this document is believed to contain correct information, neither the United States Government nor any agency thereof, nor the Regents of the University of California, nor any of their employees, makes any warranty, express or implied, or assumes any legal responsibility for the accuracy, completeness, or usefulness of any information, apparatus, product, or process disclosed, or represents that its use would not infringe privately owned rights. Reference herein to any specific commercial product, process, or service by its trade name, trademark, manufacturer, or otherwise, does not necessarily constitute or imply its endorsement, recommendation, or favoring by the United States Government or any agency thereof, or the Regents of the University of California. The views and opinions of authors expressed herein do not necessarily state or reflect those of the United States Government or any agency thereof or the Regents of the University of California.

SPE-18426

A NEW SEMI-ANALYTICAL METHOD FOR NUMERICAL SIMULATION OF FLUID AND HEAT FLOW IN FRACTURED RESERVOIRS

K. Pruess and Y. S. Wu

Earth Sciences Division
Lawrence Berkeley Laboratory
1 Cyclotron Road
Berkeley, California 94720

ABSTRACT

Permeability and flow in many petroleum, gas, and geothermal reservoirs are dominated by fractures. Despite major advances in recent years, mathematical modeling of fluid and heat flow in fractured reservoirs remains a difficult problem. Porous medium approximations have been shown to be inadequate for many flow processes in fractured systems, while double- or multiple-porosity techniques may involve excessive amounts of numerical work or large discretization errors.

We have developed a new method for modeling fluid and heat flow in fractured reservoirs which is an extension of a technique developed by Vinsome and Westerveld (1980), for calculating heat exchange between permeable layers and impermeable semi-infinite confining beds during thermally enhanced oil recovery. Our method combines a finite-difference description of global flow in the fractures with an analytical representation of interporosity flow by means of trial functions for fluid pressures and temperatures in the matrix blocks. The trial functions contain adjustable parameters which are calculated for each time step in a fully coupled way based on matrix block shapes and dimensions, utilizing simple mass and energy conservation principles.

We have incorporated the semi-analytical technique into our general-purpose multiphase simulator MULKOM. The method was verified by comparison with exact analytical solutions for fluid and heat exchange with individual matrix blocks. Applications were made to geothermal well test and production-injection problems with interporosity fluid and heat flow. The calculations show excellent agreement with numerical simulations using the method of "multiple interacting continua" (MINC), with no noticeable increase in computing work compared to porous medium calculations.

INTRODUCTION

Following pioneering work by Barenblatt et al. (1960) and Warren and Root (1963), many advances have been made in the mathematical modeling of flow in fractured porous media. In the double-porosity approach, global flow in the medium is considered to occur only through

the network of interconnected fractures, while rock matrix and fractures may exchange fluid and heat locally ("interporosity flow"). The generalization of permitting global flow through both fractures and matrix blocks has also been made (Miller and Allman, 1986; Dean and Lo, 1986). This more general method has been referred to as "dual permeability;" it can deal with multiphase flow systems in which the global flow geometry may be rather different for different phases because of capillary effects (wetting phase flowing preferentially through the blocks, non-wetting phase preferentially through the fractures; Wang and Narasimhan, 1985). There is an extensive literature describing numerical and analytical approaches to flow in fractured reservoirs. The problems treated include well testing (see the review by Gringarten, 1982), flow in fractured aquifers (Closmann, 1975; Duguid and Lee, 1977;), waterflooding of oil reservoirs (Kazemi et al., 1976; de Swaan, 1978; Menouar and Knapp, 1980), multicomponent flow (Yamamoto et al., 1971; Gilman and Kazemi, 1983; Barker, 1985), non-isothermal flow in geothermal reservoirs (Moench, 1978; O'Sullivan and Pruess, 1980; Pruess and Narasimhan, 1982, 1985; Clemo, 1985; Miller and Allman, 1986; O'Sullivan, 1987), and steamflooding of hydrocarbon reservoirs (Geshelin et al., 1981).

Many workers have made the approximation of treating the interflow between matrix and fractures as quasi-steady, with interporosity flow rate being proportional to the difference between average pressures in matrix and fractures. This approximation is usually satisfactory for isothermal single-phase flow. However, for problems involving heat exchange between matrix and fractures, and for multiphase flows with strong phase mobility effects, transient flow conditions in the blocks can persist for very long time periods (decades). Under these conditions it is necessary to represent the flow inside the blocks and at the block-fracture interface in considerable spatial detail. Closmann (1975) and Duguid and Lee (1977) used analytical techniques borrowed from the theory of heat conduction (Carslaw and Jaeger, 1959) to solve for flow with constant diffusivity in the blocks in the form of infinite series expansions. Pruess and Narasimhan (1982, 1985) developed a "multiple interacting continua" technique ("MINC"; see Fig 1), in which transient flow in the blocks and between blocks and fractures is described entirely by numerical methods, using appropriate subgridding of the blocks. The MINC approach is very flexible, and is applicable to nonisothermal multiphase flows. Because of the subgridding in the blocks, it increases the computational work by typically a factor of five in comparison to single porous medium models.

In this paper we develop a new approach for dealing with transient interporosity flow. Conceptually, the semi-analytical technique developed here is similar to the MINC-method, but it obviates the need for subgridding of matrix blocks. Thereby flow in fractured porous media can be simulated with no noticeable increase in computational work compared to simple porous medium models; furthermore, space discretization errors in the description of matrix flow are avoided. The method is an adaptation of a technique developed by Vinsome and Westerveld (1980) for describing heat exchange with impermeable confining beds in thermally enhanced oil recovery. The basic idea is to describe fluid and heat exchange between matrix blocks and fractures by semi-analytical means, using simple trial functions for temperature and pressure distributions in the matrix blocks. In a previous paper (Pruess and Wu, 1988) we presented a numerical simulation technique that incorporates a semi-analytical treatment of heat exchange with impermeable blocks; this is extended here to coupled fluid and heat exchange with matrix blocks of finite permeability.

THE METHOD OF VINSOME AND WESTERVELD

An important aspect of thermal oil recovery schemes is the transfer of heat by conduction from the reservoir to adjacent strata of low permeability. In steam and hot waterfloods this represents a heat loss which may have significant effects on process economics. In steam soak operations (huff-and-puff) heat lost to cap and base rock during injection can be partially conducted back to the reservoir during the production cycle, providing beneficial effects. The heat exchange with impermeable strata can be large and must be included in numerical simulations of thermal recovery. At early times the conductive temperature profile has rather steep gradients near the surface of the conductive zone, while at late time it extends to large distance from the boundary. A reasonably accurate representation of heat conduction by numerical methods (e.g. finite differences) therefore requires many grid blocks and can greatly increase the computational work.

A number of semi-analytical and variational approaches have been developed which permit modeling of conductive heat exchange with impermeable strata without requiring these strata to be explicitly included in the domain of a finite difference model (Weinstein, 1972, 1974; Chase and O'Dell, 1973; Vinsome and Westerveld, 1980). Of these the method of Vinsome and Westerveld is the most attractive due to its elegance and simplicity. Observing that the process of heat conduction tends to dampen out temperature variations, Vinsome and Westerveld suggested that cap- and base-rock temperatures would vary smoothly even for strong and rapid temperature changes at the boundary of the conductive zone. Arguing that heat conduction perpendicular to the conductive boundary is more important than parallel to it, they proposed to represent the temperature profile in a conductive layer by means of a simple trial function, as follows:

$$T(x,t) - T_i = (T_f - T_i + px + qx^2)e^{-x/d} \tag{1}$$

Here x is the distance from the boundary, T_i is initial temperature in cap- or base-rock (assumed uniform), T_f is the time-varying temperature at cap- or base-rock boundary, p and q are time-varying fit-parameters, and d is the penetration depth for heat conduction, defined by

$$d = \frac{\sqrt{\kappa t}}{2} \tag{2}$$

where $\kappa = K/\rho c$ is the thermal diffusivity, K the thermal conductivity, ρ the density of the medium, and c the specific heat. In connection with a finite-difference simulation of non-isothermal flow, each grid block in the top and bottom layers of the computational grid will have an associated temperature profile in the adjacent impermeable rock as given by Eq. (1). The coefficients p and q will be different for each grid block; they are determined concurrently with the flow simulation from simple physical principles, namely: (1) temperature at the conductive boundary obeys the heat conduction equation for the impermeable stratum, and (2) the rate of change in total cap- or base-rock heat content is equal to the heat flux at the boundary. Vinsome and Westerveld presented test calculations which showed that their method was able to accurately represent monotonic as well as non-monotonic temperature profiles. We incorporated their technique into our MULKOM simulator (Pruess, 1983b, 1988) and verified that it gave accurate results (Pruess and Bodvarsson, 1984).

HEAT EXCHANGE WITH BLOCKS OF IMPERMEABLE ROCK

The method of Vinsome and Westerveld treats heat exchange between a surface with time varying temperature and a semi-infinite conductive half-space. It can be easily adapted to the problem of heat exchange between impermeable rock matrix blocks and fluids flowing in fractures or porous materials around these blocks. The required modifications involve the equation of heat conduction and the calculation of total heat content in the blocks, both of which differ from those for a semi-infinite medium.

Following concepts developed in the method of "multiple interacting continua" or "MINC" (see Fig. 1) we approximate heat flow in impermeable blocks of rock as being one-dimensional, with temperatures in the blocks depending only on the distance x from the nearest block surface (i.e. from the nearest fracture; Pruess and Narasimhan, 1982, 1985). We use the concept of "proximity function" (Pruess and Karasaki, 1982) to describe one-dimensional flow in blocks of arbitrary shape, as well as flow in stochastic assemblages of matrix blocks which are encountered in fractured reservoirs. For matrix blocks of volume V_m having a volume V(x) within a distance x from the fractures (i.e., from the block surfaces), the proximity function is defined as:

$$\mathrm{PROX}(x) = \frac{V(x)}{V_m} \tag{3}$$

The interface area for flow in the matrix blocks at distance x from the surface is

$$A(x) = \frac{dV}{dx} = V_m \, d\frac{\mathrm{PROX}}{dx} \tag{4}$$

Considering a heat balance for a volume element dV = A(x) dx, we obtain the following equation for one-dimensional heat conduction in the blocks:

$$\frac{\partial T}{\partial t} = \kappa \frac{\partial^2 T}{\partial x^2} + \kappa \frac{\partial T}{\partial x} \frac{\partial \ln A}{\partial x} \tag{5}$$

Choosing the same form Eq. (1) for the temperature profile in the blocks as was used by Vinsome and Westerveld for the semi-infinite solid, the condition that Eq. (5) must be satisfied at the surface of the blocks gives

$$\frac{T_f - T_f^o}{\kappa \Delta t} = \frac{\theta}{d^2} - \frac{2p}{d} + 2q + \left.\frac{d\ln A}{dx}\right|_0 \left(p - \frac{\theta}{d}\right) \tag{6}$$

Here we have replaced the time derivative by a first-order forward finite difference, as required for incorporating the method into our numerical simulator MULKOM. T_f^o and T_f are temperatures in the fracture at the beginning and end of the time step Δt, respectively. θ is an abbreviation for T_f - T_i. For a semi-infinite solid the derivative term involving A(x) vanishes, so that Eq. (6) then reduces to the form given by Vinsome and Westerveld. Energy conservation in the blocks is expressed as follows.

$$\frac{d}{dt} \int_{V_m} \rho c T dV = -K \left.\frac{\partial T}{\partial x}\right|_0 A(x=0) \tag{7}$$

With a slight rearrangement of terms the integral on the left hand side becomes

$$I(t) = \int_0^{L/2} [T(x,t) - T_i] \frac{A(x)}{A(0)} dx \tag{8a}$$

The integration extends to L/2, which for fracture spacing L is the largest distance from the block surfaces. Inserting Eq. (1), this integral can be written as

$$I(t) = \beta q + \gamma p + \delta\theta \tag{8b}$$

The coefficients β, γ and δ represent a weighting of the x-dependent terms $x^n \exp(-x/d)$ (n = 0, 1, 2) with the function A(x)/A(0) characterizing the matrix block shapes. Even for irregular blocks and stochastic assemblages, the proximity function and its derivative A(x) can be written as polynomials in x (Pruess and Karasaki, 1982), so that the integral in Eq. (8) can be evaluated by elementary means. Evaluating the spatial derivative from Eq. (1) the finite difference version of Eq. (7) becomes

$$\kappa\Delta t \left(\frac{\theta}{d} - p\right) = I(t+\Delta t) - I(t) \tag{9}$$

Eqs. (6) and (9) (with the definition Eq. 8) represent two linear equations for the two unknown time-dependent parameters p and q. Solution of these is trivial once the coefficients β, γ, and δ in Eq. (8b) have been obtained. The heat flux from the blocks to the fractures is calculated as in Vinsome/Westerveld by

$$Q = K \left.\frac{\partial T}{\partial x}\right|_0 = -K \left(\frac{\theta}{d} - p\right) \tag{10}$$

Calculation of the time-dependent coefficients p and q from Eqs. (6) and (9), and of heat exchange between the permeable and the conductive domains from Eq. (10), has to be done at each time step separately for all grid blocks which contain purely conductive material. It is possible to apply the conductive exchange calculation only for certain grid blocks, while others may be treated as homogeneous porous media, or as fractured media with permeable matrix using the MINC method. The temperature T (x = 0, t) at the surface of the conductive domain is identified with the temperature in the permeable portion (fractures) of the grid block. In a fully implicit scheme this temperature is evaluated at the new time level t + Δt, and the heat exchange calculation is done in a fully coupled manner as part of the iterative process to solve the fluid and heat flow equations in the permeable domain.

To incorporate the above scheme into a numerical simulator we partition grid block volumes into a permeable and a purely conductive part:

$$V_n = V_{n,per} + V_{n,cond} \tag{11}$$

Fluid and heat flow in the permeable portions $V_{n,per}$ of the grid blocks is handled by numerical simulation. Heat transferred by conduction from the impermeable portion $V_{n,cond}$ is represented by including Eq. (10), properly scaled for the total block surface area in V_n, as a source term into the heat balance equation for $V_{n,per}$.

EVALUATION

We have implemented the method described in the foregoing section into our general purpose simulator MULKOM, and have performed several tests and comparisons. For simplicity this was done for matrix blocks of cubic shape. For cubes the proximity function can be directly obtained from the definition Eq. (3); it is given by

$$\mathrm{PROX}(x) = \frac{6x}{L} - \frac{12x^2}{L^2} + \frac{8x^3}{L^3} \tag{12}$$

This leads to a particularly simple form for the expression A(x)/A(0) appearing in the integral Eq. (8), namely,

$$\frac{A(x)}{A(0)} = \left[1 - \frac{2x}{L}\right]^2 \tag{13}$$

In order to evaluate the accuracy of the semi-analytical approximation we have studied a problem for which exact analytical solutions are available, namely, heat exchange with a cube of initially uniform temperature, which at time t = 0 is subjected to a step change in temperature at the surface. The parameters of the problem are given in Table 1.

Table 1. Parameters for test problem (heat exchange with unit cube).

side length of cube	1 m
rock density	2650 kg/m^3
specific heat	1000 J/kg°C
heat conductivity	2.1 W/m°C
initial temperature	300°C
surface temperature for t > 0	100°C

The heat flow rate at the surface of the cube was computed as function of time using the following four approaches: (1) numerical evaluation of the exact three-dimensional Fourier series solution (Carslaw and Jaeger, 1959); (2) a one-dimensional approximation to heat flow in a cube, for which the exact solution is identical to heat flow in a sphere (Carslaw and Jaeger, 1959); (3) the semi-analytical solution as developed above, incorporated into the MULKOM simulator; and (4) method of multiple interacting continua ("MINC"; Pruess and Narasimhan, 1985). Results from the different approaches are given in tabular form (Tables 2 and 3), because they agree so closely as to be almost indistinguishable when plotted as rate versus time on log-log paper.

Table 2. Heat flow rates from unit cube.

Time (s)	Heat Flow Rate (W)			
	exact 3-D	exact 1-D	semi-analytical	MINC
1	1.410E6	1.592E6	1.821E6	1.315E6
10	4.987E5	5.000E5	5.038E5	6.122E5
10^2	1.534E5	1.547E5	1.546E5	1.683E5
10^3	4.429E4	4.547E4	4.514E4	4.913E4
10^4	1.020E4	1.093E4	1.063E4	1.207E4
10^5	6.354E2	4.414E2	9.478E2	8.372E2
10^6	4.275E-7	2.610E-10	1.021E1	5.676E-2

Table 3. Cumulative heat flows from unit cube.

Time (s)	Cumulative Conductive Heat Transfer (MJ)			
	exact 3-D	exact 1-D	semi-analytical	MINC
1	3.285	3.286	2.645	1.22
10	10.04	10.05	9.079	8.52
10^2	31.31	31.44	28.40	30.28
10^3	94.73	95.97	86.09	93.52
10^4	259.6	269.0	235.7	261.8
10^5	503.0	515.9	453.9	503.3
10^6	530.0	530.0	524.9	529.9

The "exact 3-D" and the "exact 1-D" results are virtually identical, with the exception of very early and very late times, which have little significance for overall heat transfer. Heat flow rates calculated in the semi-analytical approximation agree very well with the exact results, being typically 1-2 % larger. Cumulative heat transfer in the semi-analytical approximation is underpredicted by typically 10% at most times, but it approaches the correct asymptotic value of 5.3×10^8 J at late times. It may appear inconsistent that heat flow rates in the semi-analytical approximation are slightly on the high side at all times while cumulative heat transfer is somewhat low. This effect is caused by the relatively coarse time stepping in the numerical simulations. In the semi-analytical approach the heat flow rate is constant during each time step; moreover, in our fully implicit scheme it is equal to the heat flow rate at the end of the time step. Because heat flow rates are monotonically declining this leads to some underprediction of cumulative heat transfer. The accuracy of the semi-analytical calculation could be improved by taking smaller time steps (we used 4 time steps per log-cycle), or by using a mid-point weighting in time (Crank-Nicolson equation; Peaceman, 1977) rather than a fully implicit treatment. However, in practical problems one is seldom interested in accurate answers

over many orders of magnitude in time, so that time steps do not need to grow as fast as in our test case, and better time truncation accuracy will be attainable.

Heat flow rates calculated in the MINC approach, using 50 subcontinua of equal volume, differ by as much as 10 - 20% from the exact values. For rates that change with time by many orders of magnitude this is not at all a bad approximation. In terms of cumulative heat transfer the MINC approximation does extremely well (Table 3). After a brief period with significant space discretization effects at very early times, the MINC results agree with the exact solution to better than 1%.

FIVE–SPOT

We have applied the semi-analytical heat exchange approach to a two-dimensional five-spot production/injection problem similar to that previously studied by Pruess (1983a). Problem parameters are given in Table 4.

Table 4. Specifications of five-spot problem.

Formation	
rock grain density	2650 kg/m^3
specific heat	1000 J/kg°C
heat conductivity	2.1 W/m°C
permeable volume fraction	2%
porosity in permeable domain	50%
impermeable blocks: cubes with side length	50 m, 250 m
effective permeability	6.0×10^{-15}m^2
thickness	305 m
relative permeability: Corey curves with $S_{lr} = 0.30$, $S_{vr} = 0.05$	
initial temperature	300°C
initial liquid saturation	0.99
initial pressure	85.93 bar
production/injection	
pattern area	1 km^2
distance between producers and injectors	707.1 m
production rate (*)	30 kg/s
injection rate (*)	30 kg/s
injection enthalpy	500 kJ/kg

(*) full-well basis

The grid used in the numerical simulations represents 1/8 of a five-spot; it has six rows and

eleven columns for a total of thirty-six volume elements (see Fig. 2). We assume three sets of equidistant, plane, parallel fractures at right angles, so that the impermeable matrix blocks are cubes. Calculations were done for two different fracture spacings. In addition to using the semi-analytical approach we also performed simulations with the MINC method, and with a uniform porous medium model (with same total void space, i.e., porosity of 1%). The MINC approach uses five subcontinua, with volume fractions of .02, .08, .20, .35, and .35. Results are given in Figure 3 and in Table 5.

Fig. 3 shows temperature profiles along the line connecting a producer and an injector after 36.5 years, corresponding to injection of approximately 12.2 pore volumes. For both fracture spacings the agreement between the semi-analytical and the MINC simulations is excellent. The D = 50 m results are indistinguishable from the porous medium calculation, while at the larger fracture spacing of D = 250 m the thermal sweep is less complete and lower temperatures are obtained. Predicted total heat transfer from the impermeable rocks to the fluids agrees to better than 1% between the semi-analytical and MINC approaches at most times (see Table 5). The semi-analytical approach required the same amount of computing time as the porous medium case, while the MINC calculation was approximately five times slower.

Table 5. Cumulative heat transfer from rocks to fluids in 1/8 of five-spot.

Time (years)	Cumulative Conductive Heat Transfer (10^{14} J)			
	Fracture Spacing 50 m		Fracture Spacing 250 m	
	MINC	Semi-analytical	MINC	Semi-analytical
1	1.07	1.07	.83	.85
2	2.11	2.10	1.77	1.79
5	5.22	5.18	4.64	4.67
10	10.33	10.29	9.40	9.46
15	15.48	15.44	14.10	14.16
20	20.43	20.38	18.70	18.79
25	25.24	25.19	23.21	23.33
30	30.14	30.10	27.60	27.75
35	35.05	35.00	31.91	32.07

PERMEABLE MATRIX BLOCKS

The isothermal flow of single-phase fluid with small and constant compressibility is governed by the same diffusion equation as is heat conduction, so the treatment developed above is immediately applicable for this case. New issues arise in non-isothermal flow, because pressure diffusivity $\lambda = \frac{k}{\phi\zeta\mu}$ and fluid density ρ depend strongly and in non-linear fashion on temperature. In complete analogy to Eq. (1), we write the fluid pressure in the matrix blocks as

$$P(x,t) - P_i = (P_f - P_i + rx + sx^2)\, e^{-x/D} \tag{14}$$

where $D = \frac{\sqrt{\lambda t}}{2}$ is the penetration depth for a pressure disturbance at the block surface. This will be evaluated at original block temperature, because pressure penetration tends to run ahead of temperature penetration in most cases of practical interest. Indeed, even for very tight matrix blocks with $k = 10^{-18}\,m^2$ and a large compressibility of $10^{-9}\,Pa^{-1}$, with a porosity of 10% and a viscosity of water at ambient temperature of 10^{-3} Pa.s, pressure diffusivity $\lambda = 10^{-5}\,\frac{m^2}{s}$ is an order of magnitude larger than typical thermal diffusivities of rocks. At late time fracture temperatures will of course penetrate all the way into the blocks. However, at that time D >> L, so that the precise temperature choice for evaluating D becomes immaterial. From the requirement that the fluid flow analog of Eq. (5) be satisfied at the block surface, we obtain the counterpart of Eq. (6)

$$\frac{P_f - P_f^o}{\lambda_f \Delta t} = \frac{\sigma}{D^2} - \frac{2r}{D} + 2s + \frac{\partial \ln A}{\partial x}\bigg|_0 (r - \frac{\sigma}{D}) \tag{15}$$

Here we have abbreviated $\sigma = P_f - P_i$. The index f on the pressure diffusivity λ_f indicates that this quantity is to be evaluated at block surface conditions (T_f, P_f). In analogy to Eq. (7), mass conservation in the blocks is written as

$$\frac{d}{dt}\int_{V_m} \phi\rho dV = -k(\frac{\rho}{\mu})_f \frac{\partial P}{\partial x}\bigg|_0 A(x=0) \tag{16}$$

where fluid mobility $k(\rho/\mu)_f$ is also evaluated at the block surface. When pressure and temperature changes are large, ρ in the integral in Eq. (16) could vary in highly non-linear fashion. In order to obtain a calculationally efficient method we insist on evaluating the integral analytically, and we therefore restrict ρ and ϕ to a linear dependence, as follows:

$$\rho(T,p) = \rho_i\Big[1 - \varepsilon_l(T - T_i) + \zeta_l(P - P_i)\Big] \tag{17a}$$

$$\phi(T,p) = \phi_i\Big[1 - \varepsilon_R(T - T_i) + \zeta_R(P - P_i)\Big] \tag{17b}$$

Inserting this in Eq. (16) and retaining only first-order terms, we obtain the counterpart of Eq. (9) for nonisothermal fluid flow as

$$\frac{k}{\phi_i\rho_i}(\frac{\rho}{\mu})_f \Delta t(\frac{\sigma}{D} - r) = \zeta\Big[J(t + \Delta t) - J(t)\Big] - \varepsilon\Big[I(t + \Delta t) - I(t)\Big] \tag{18}$$

Here we have introduced the finite-difference version of the pressure derivative term in Eq. (16). J denotes an integral of the form Eq. (8a), with temperature replaced by pressure. $\zeta = \zeta_l + \zeta_R$ and $\varepsilon = \varepsilon_l + \varepsilon_R$ are total compressibility and expansivity, respectively.

Equations (15) and (18) are two coupled equations for the parameters r and s of the pressure expansion function Eq. (14) in the blocks. Through the integrals I these are coupled to the temperature distributions, with coupling strength proportional to expansivity ε. In our implementation in the MULKOM simulator we first calculate, at each step of the Newton-Raphson iteration process, the temperature parameters p and q from Eqs. (6) and (9). These are then used to evaluate the integral I from Eq. (8a), which is substituted into Eq. (18), and subsequently the pressure parameters r and s are calculated from Eqs. (15) and (18). The fluid flux from the blocks to the fractures is obtained by differentiating Eq. (14), as follows:

$$F = k(\frac{\rho}{\mu})_f \frac{\partial p}{\partial x}\bigg|_0 = -k(\frac{\rho}{\mu})_f(\frac{\sigma}{D} - r) \tag{19}$$

The fluid exchange will also give rise to a sensible-heat term in the heat balance equation. This term was found to be negligibly small for single-phase water. All interporosity flow terms are calculated in MULKOM in a fully coupled and implicit manner during the simulation.

TEST CALCULATIONS

We have evaluated the accuracy of the coupled fluid and heat exchange scheme by considering an idealized problem involving a single matrix block surrounded by a finite-volume fracture (see Fig. 4). Initially, both domains contain single-phase water at greatly different temperatures and pressures. The parameters for this problem as given in Table 6 can be considered representative of conditions that may typically be encountered in geothermal injection operations. The process of pressure and temperature equilibration was simulated using the semi-analytical approximation, and results were compared with MINC-calculations employing very fine subgridding of the matrix block.

Table 6. Specifications for single-block fluid and heat exchange.

MATRIX DATA		
cube size	$10 \times 10 \times 10\,m^3$	
permeability	$10^{-17}\,m^2$ (10 μd)	
porosity	5 %	
compressibility	$10^{-9}\,Pa^{-1}$	
rock grain density	$2650\,kg/m^3$	
specific heat	1000 J/kg °C	
heat conductivity	2.1 W/m °C	
FRACTURE DATA		
	Case 1	Case 2
volume fraction	0.5	0.1
porosity in fracture domain	5%	5%
INITIAL CONDITIONS		
	Case 1 (T,P)	Case 2 (T,P)
fractures	(100 °C, 100 bar)	(100 °C, 150 bar)
matrix	(240 °C, 50 bar)	(240 °C, 100 bar)

During initial test calculations it became apparent that thermal expansion effects on water density are so large and temperature dependent that a substantial improvement over the relationship Eq. (17a) with constant expansivity and compressibility was needed. The thermal expansion coefficient of water is large, in the sense that modest temperature changes in a system held at constant total fluid density will produce very large pressure effects. Indeed, in a closed system the relationship between pressure and temperature changes during equilibration is determined by

$$d\rho = \rho_i(\zeta_l dP - \varepsilon_l dT) \overset{!}{=} 0 \tag{20}$$

so that

$$\frac{dP}{dT} = \frac{\varepsilon_l}{\zeta_l} \tag{21}$$

with typical values of 5.0 bar/°C at (T, P) = (100 °C, 100 bar), and increasing with temperature to 7.8 bar/°C at (T,P) = (240 °C, 50 bar). The substantial increase of the ratio $\frac{\varepsilon_l}{\zeta_l}$ with temperature produces interesting effects during thermal equilibration of waters of different temperature. The pressure drop experienced by the hotter water in the matrix from thermal contraction outweighs the pressure increase of the colder water in the fractures from thermal expansion. As a consequence, mixture pressures tend to equilibrate at rather low values. Because of the pronounced temperature dependence of both expansivity and compressibility Eq. (17a) is a poor approximation. Initial calculations with the semi-analytical method gave rather inaccurate pressure predictions, that were tens of bars too high. This could be remedied by using time-dependent expansivity and compressibility in Eq. (17a), evaluated at average block temperature, which can be obtained during a simulation from known parameters as follows:

$$\bar{T}_m(t) = T_i + \frac{6}{L} I(t) \tag{22}$$

Results for the two single-block problems are shown in Figures 5 and 6. In Case 1 there is excellent agreement between semi-analytical and MINC approximations for both pressures and temperatures over many log-cycles in time. For $t > 10^5$ s the pressure drop calculated from the MINC method flattens out; associated with this is a faster temperature rise in the MINC calculation. Closer inspection indicated that these phenomena were caused by the emergence of two-phase (steam-water) conditions deep in the matrix block, where temperatures were still high (approximately 240 °C), while pressures had declined down to the saturated vapor pressure. These phase change and two-phase flow effects are not represented in the semi-analytical approach. It should be pointed out that these effects are unlikely to occur in practical circumstances, where the fracture domain would be connected to a larger reservoir volume and would in fact be pressurized from injection operations.

An attempt was made to generate other cases in which no phase transitions would occur. In order to diminish the strong pressure decline resulting from thermal equilibration of waters of 240 °C and 120 °C, respectively, we reduced the relative volume of the fracture domain to 10 % (Case 2, Table 6). (Note that in realistic cases fractures will typically represent at most a few percent of reservoir volume.) This results in an equilibration temperature of 226 °C, much closer to the original matrix temperature than in Case 1. Results for this case are shown in Figure 6. Semi-analytical and MINC temperatures now agree very well over the entire equilibration process, while pressure agreement is less close at early times. This is caused by the reduction in fracture volume which amplifies the pressure effects from temperature changes in

the blocks. It is significant that there is never any pressure excursion. In both cases equilibrium temperatures and pressures show excellent agreement between semi-analytical and MINC-results.

When comparing results from the semi-analytical and MINC calculations, one must keep in mind the extreme sensitivity of water pressures to small density changes. From the level of pressure agreement shown in Figures 5 and 6 it can be concluded that the interporosity fluid and heat flow rates calculated from the semi-analytical approximation agree very closely with those predicted from the MINC method. Note also that in actual reservoir problems the sensitivity to small inaccuracies in individual block response will be much reduced from global flow effects.

ONE–DIMENSIONAL RADIAL FLOW

The semi-analytical fluid and heat exchange technique was applied to model cold water injection into a fractured-porous formation in one-dimensional radial flow geometry. The problem parameters as given in Table 7 are representative of typical geothermal injection problems in single-phase liquid reservoirs. Matrix blocks were assumed to be cubes, and a wide range of block sizes was studied. Figure 7 shows that pressure buildups calculated with the semi-analytical representation of interporosity flow agree very well with results obtained from the MINC method. The buildup for permeable blocks displays varying curvature with no straight-line segments. It had been observed previously that nonisothermal injection into fractured media shows very complex behavior that appears to defy simple analysis methods (O'Sullivan, 1987, and references therein).

Temperature profiles after 49.3 days of injection are plotted in Figure 8. It is observed that for small matrix block sizes reservoir response approaches the uniform porous medium limit, as expected. For very large block sizes the surface-to-volume ratio asymptotes to zero, so that reservoir behavior should again approach a porous medium limit, but corresponding to only the fracture domain being present. This is confirmed by the results plotted in Figures 8 and 9. Note that most of the width of the temperature fronts for the porous medium limits is due to numerical dispersion; thermal fronts in a uniform porous medium are known to be sharp, except for rather small heat conduction effects (Bodvarsson, 1972). The broad thermal fronts observed for injection into fractured media are "real", being caused by the delayed heat transfer from the blocks to the fractures.

Figure 10 shows simulated pressure falloff and temperature buildup in response to shutting in the injection well after 11.6 days. Notice that pressure response is insensitive to matrix block size while temperature transients depend strongly on block size. This suggests that useful information on fracture spacings may be obtainable from temperature monitoring following non-isothermal injection.

Table 7. Specifications of one-dimensional radial injection problem

FORMATION DATA		
thickness	100 m	
permeability	$50 \cdot 10^{-15}$ m^2	(50 md)
average fracture porosity	1 %	
matrix blocks: cubes		
block volumes (range)	$1 - 10^{12}$ m^3	
matrix permeability	10^{-17} m^2	(10 μd)
matrix porosity	8 %	
pore compressibility	10^{-9} Pa^{-1}	
rock grain density	2600 kg/m^3	
rock specific heat	920 J/kg °C	
formation heat conductivity	2.51 W/m °C	
INITIAL CONDITIONS		
temperature	240 °C	
pressure	100 bar	
WELL CONDITIONS		
fully penetrating		
wellbore radius	0.1 m	
injection rate	37.5 kg/s	
injection enthalpy	500 kJ/kg	

DISCUSSION AND CONCLUSIONS

We have incorporated an analytical interporosity flow model into a numerical simulator to calculate fluid and heat exchange between matrix blocks of low permeability and fluids migrating past these blocks in fractures. Our method uses simple trial functions to represent flow inside the matrix blocks and across matrix block surfaces. This offers a means of simulating fluid and heat flow in fractured media with no noticeable increase in computing work as compared to porous medium simulations. Detailed analysis of heat flow from a cube suggested that the semi-analytical approximation should provide good accuracy. Simulations for a two-phase production/injection problem with phase change and for radial flow in nonisothermal injection gave almost perfect agreement with the MINC method.

The reason why the semi-analytical method performs even better on reservoir problems than might have been expected from the test results for an individual matrix block is in the nature of the interplay between global and interporosity flow. Namely, the aggregate response of many rock blocks in a reservoir flow problem tends to compensate for inaccuracies that may be present in the modeling of individual block response. To see how this comes about, suppose that because of discretization effects the blocks near the injection well do not deliver heat to the fluids as rapidly as they should. (This is what actually happens in the heat exchange problem tabulated in Table 3.) As a consequence fluids will have somewhat lower temperatures when at later time they sweep past downstream blocks, and hence they will pick up more heat from those blocks. This compensation of inaccuracies in individual block response from global reservoir mechanisms is completely analogous to what was observed in analysis of waterfloods in fractured hydrocarbon reservoirs (Wu and Pruess, 1988). It indicates that satisfactory accuracy in reservoir flow problems should be attainable with rather modest accuracy requirements for individual blocks.

A somewhat different approach for approximating the response of matrix blocks to changing boundary conditions at the block surfaces was recently developed by Zimmerman and Bodvarsson (1988). These authors constructed trial functions based on early and late time block response, and showed that such functions can provide good engineering accuracy for representing flow rates at matrix block surfaces. The Zimmerman and Bodvarsson trial functions should be capable of producing good accuracy for reservoir-type simulation problems with global fracture flow, but no such implementation has been reported yet.

The semi-analytical treatment of interporosity flow as presented in this paper is applicable to multiphase fluid and heat flow problems with impermeable matrix blocks (heat exchange only), and for single phase fluid and heat flow problems with permeable matrix blocks (coupled fluid and heat exchange). For single phase flow problems involving gas instead of liquid the trial function for fluid pressure, Eq. (14), would be written in terms of P^2 instead of P. The method can also be applied to problems of chemical transport in fractured media, because chemical transport in low-permeability blocks of rock can be described in analogy to heat conduction. The problem of multiphase fluid and heat exchange with permeable blocks is considerably more difficult. In addition to trial functions for temperature and pressure this will require an approximate representation of saturation distributions in the blocks. Work along these lines is in progress.

ACKNOWLEDGEMENT

For a critical review of the manuscript the authors are grateful to R. W. Zimmerman and J. Noorishad. This work was supported by the Geothermal Technology Division, U.S. Department of Energy, under Contract No. DE-AC03-76SF00098.

NOMENCLATURE

A	area, m^2
c	heat capacity, J/kg °C
d	penetration depth for heat conduction, m
D	penetration depth for fluid flow, m
F	fluid flux, $kg/m^2 \cdot s$
I	temperature integral, defined in Eq. (8a), °C · m
J	pressure integral, Pa · m
k	permeability, m^2
K	heat conductivity, W/m · °C
L	side length of cube, m
p	parameter in temperature expansion, Eq. (1)
P	pressure, Pa or bar ($\equiv 10^5$ Pa)
PROX	proximity function, dimensionless
q	parameter in temperature expansion, Eq. (1)
Q	heat flux, W/m^2
r	parameter in pressure expansion, Eq. (14)
s	parameter in pressure expansion, Eq. (14)
t	time, s
T	temperature, °C
V	volume, m^3
x	distance from block surface, m

GREEK

β	
γ	geometric coefficients in temperature integral, Eq. (8b)
δ	
θ	temperature change in fractures, °C
κ	thermal diffusivity, m^2/s
λ	pressure diffusivity, m^2/s
ρ	density, kg/m^3
ε	expansivity, $°C^{-1}$

ζ	compressibility, Pa^{-1}
μ	viscosity, $Pa \cdot s$
σ	pressure change in fractures, Pa

SUBSCRIPTS

cond	conductive
f	fracture
i	initial
l	liquid
m	matrix
n	grid block index
per	permeable
R	rock

REFERENCES

Barenblatt, G. E., Zheltov, I. P. and Kochina, I. N., (1960), Basic Concepts in the Theory of Seepage of Homogeneous Liquids in Fissured Rocks, *J. Appl. Math., USSR*, Vol. 24, No. 5, pp. 1286-1303.

Barker, J. A., (1985), Block-Geometry Functions Characterizing Transport in Densely Fissured Media, *J. of Hydrology*, Vol. 77, pp. 263-279.

Bodvarsson, G., (1972), Thermal Problems in the Siting of Reinjection Wells, *Geothermics*, Vol. 1, No. 2, pp. 63-66.

Carslaw, H. S., and Jaeger, J. C. (1959), *Conduction of Heat in Solids*, Oxford University Press, Oxford, England, Second Edition.

Chase, C. A. and O'Dell, P. M. (1973), "Application of Variational Principles to Cap and Base Rock Heat Losses," *Trans. AIME*, Vol. 225, pp. 200-210.

Clemo, T. M., (1985), FRACSL Code Development and Correlation of East Mesa Test Results, Proc., Tenth Workshop Geothermal Reservoir Engineering, Stanford University, pp. 287-292, Stanford, CA.

Closmann, P. J., (1975), An Aquifer Model for Fissured Reservoirs, *Soc. Pet. Engr. J.*, pp. 385-398.

Dean, R. M. and Lo, L. L., (1986), Development of a Natural Fracture Simulator and Examples, paper SPE-14110, presented at the SPE 1986 International Meeting on Petroleum Engineering, Beijing, China.

de Swaan, A., (1978), Theory of Waterflooding in Fractured Reservoirs, *Soc. Pet. Engr. J.*, pp. 117-122.

Duguid, J. O. and Lee, P. C. Y., (1977), Flow in Fractured Porous Media, *Water Resour. Res.*, Vol. 13, No. 3, pp. 558-566.

Geshelin, B. M., Grabowski, J. W. and Pease, E. C., (1981), Numerical Study of Transport of Injected and Reservoir Water in Fractured Reservoirs During Steam Simulation, paper SPE 10322, presented at 56th Annual Fall Technical Conference and Exhibition of the SPE, San Antonio, TX.

Gilman, J. R. and Kazemi, H., (1983), Improvements in Simulation of Naturally Fractured Reservoirs, *Soc. Pet. Engr. J.*, pp. 695-707.

Gringarten, A. C., (1982), Flow-test Evaluation of Fractured Reservoirs, in: T. N. Narasimhan (ed.), Recent Trends in Hydrogeology, Special Paper 189, The Geological Society of America, Boulder, CO, pp. 237-263.

Kazemi, M., Merrill, Jr., L. S., Porterfield, K. L. and Zeman, P. R., (1976), Numerical Simulation of Water-Oil Flow in Naturally Fractured Reservoirs, *Soc. Pet. Engr. J.*, pp. 317-326.

Menouar, H. and Knapp, R. M., (1980), Numerical Simulation of the Imbibition Process in Fractured Reservoirs, paper SPE-9370, presented at the 55th Annual Fall Technical

Conference and Exhibition of the SPE, Dallas, TX.

Miller, J. D. and Allman, D. W., (1986), Dual Permeability Modeling of Flow in a Fractured Geothermal Reservoir, Proc., Eleventh Workshop Geothermal Reservoir Engineering, Stanford University, Stanford, CA, pp. 77-84.

Moench, A. F., (1978), The Effect of Thermal Conduction Upon Pressure Drawdown and Build-up in Fissured, Vapor-Dominated Reservoirs, Proc., Fourth Workshop on Geothermal Reservoir Engineering, Stanford University, Stanford, California.

O'Sullivan, M. J., (1987), Aspects of Geothermal Well Test Analysis in Fractured Reservoirs, *Transport in Porous Media*, Vol. 2, No. 5, pp. 497-517.

O'Sullivan, M. J. and Pruess, K., (1980), Analysis of Injection Testing of Geothermal Reservoirs, Transactions, Geothermal Resources Council, Vol. 4, pp. 401-404.

Peaceman, D. W. (1977), *Fundamentals of Numerical Reservoir Simulation*, Elsevier, Amsterdam.

Pruess, K. (1983a), Heat Transfer in Fractured Geothermal Reservoirs with Boiling, *Water Resour. Res.*, Vol. 19, No. 1, pp. 201-208.

Pruess, K. (1983b), Development of the General Purpose Simulator MULKOM, Annual Report 1982, Earth Sciences Division, Report LBL-15500, Lawrence Berkeley Laboratory.

Pruess, K. (1988), SHAFT, MULKOM, TOUGH, *Geotermia, Rev. Mexicana Geoenergia*, Vol. 4, No. 1, pp. 185-202, (also: Lawrence Berkeley Laboratory report LBL-24430, Berkeley, CA.)

Pruess, K. and Bodvarsson, G. S. (1984), Thermal Effects of Reinjection in Geothermal Reservoirs with Major Vertical Fractures, *Journal of Petroleum Technology*, Vol. 36, No. 10, pp. 1567-1578.

Pruess, K. and Karasaki, K. (1982), Proximity Functions for Modeling Fluid and Heat Flow in Reservoirs with Stochastic Fracture Distributions, presented at Eighth Workshop on Geothermal Reservoir Engineering, Stanford University, Stanford, CA.

Pruess, K. and Narasimhan, T. N. (1982), On Fluid Reserves and the Production of Superheated Steam from Fractured, Vapor-Dominated Geothermal Reservoirs, *Journal of Geophysical Research*, Vol. 87, No. B11, pp. 9329-9339.

Pruess, K. and Narasimhan, T. N. (1985), A Practical Method for Modeling Fluid and Heat Flow in Fractured Porous Media, *Soc. Pet. Engr. J.*, Vol. 25, No. 1, pp. 14-26.

Pruess, K. and Wu, Y. S., (1988), A Semi-Analytical Method for Heat Sweep Calculations in Fractured Reservoirs, presented at Thirteenth Workshop on Geothermal Reservoir Engineering, Stanford University, (LBL-24463).

Vinsome, P. K. W., and Westerveld, J. (1980), A Simple Method for Predicting Cap and Base Rock Heat Losses in Thermal Reservoir Simulators, *J. Canadian Pet. Tech.*, pp. 87-90.

Wang, J. S. Y. and Narasimhan, T. N., (1985), Hydrologic Mechanisms Governing Fluid Flow in a Partially Saturated, Fractured, Porous Medium, *Water Resour. Res.*, Vol. 21, No. 12, pp. 1861-1874.

Warren, J. E. and Root, P. J., The Behavior of Naturally Fractured Reservoirs, *Soc. Pet. Engr. J.*, pp. 245-255, also: Transactions, AIME, 228.

Weinstein, H. G., (1972), Semi-Analytic Method for Thermal Coupling of Reservoir and Overburden, *Soc. Pet. Engr. J.*, pp. 439-447.

Weinstein, H. G., (1974), Extended Semi-Analytical Method for Increasing and Decreasing Boundary Temperature, *Soc. Pet. Engr. J.*, pp. 152-164.

Wu, Y. S. and Pruess, K. (1988), A Multiple-Porosity Method for Simulation of Naturally Fractured Petroleum Reservoirs, *SPE Reservoir Engineering*, pp. 327-336.

Yamamoto, R. H., Padgett, J. D., Ford, W. T. and Boubeguira, A., (1971), Computational Reservoir Simulator For Fissured Systems — The Single Block Model, *Soc. Pet. Engr. J.*, pp. 113-129.

Zimmerman, R. W. and Bodvarsson, G. S., (1988), Integral Method Solution For Diffusion into a Spherical Block, Lawrence Berkeley Laboratory report LBL-26020, submitted for publication to *J. of Hydrology*, September 1988.

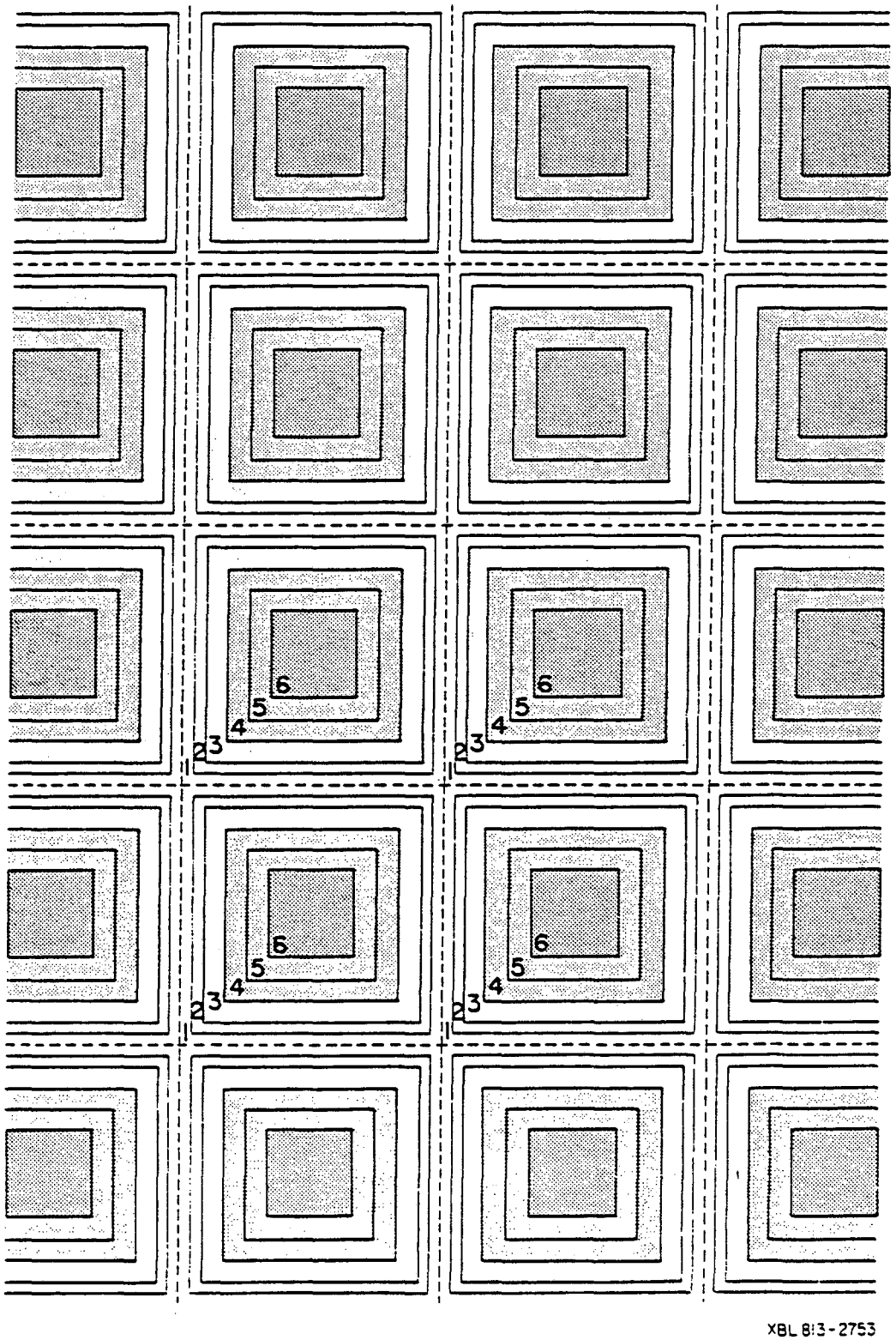

Figure 1. The concept of multiple interacting continua (MINC) for an idealized fracture system.

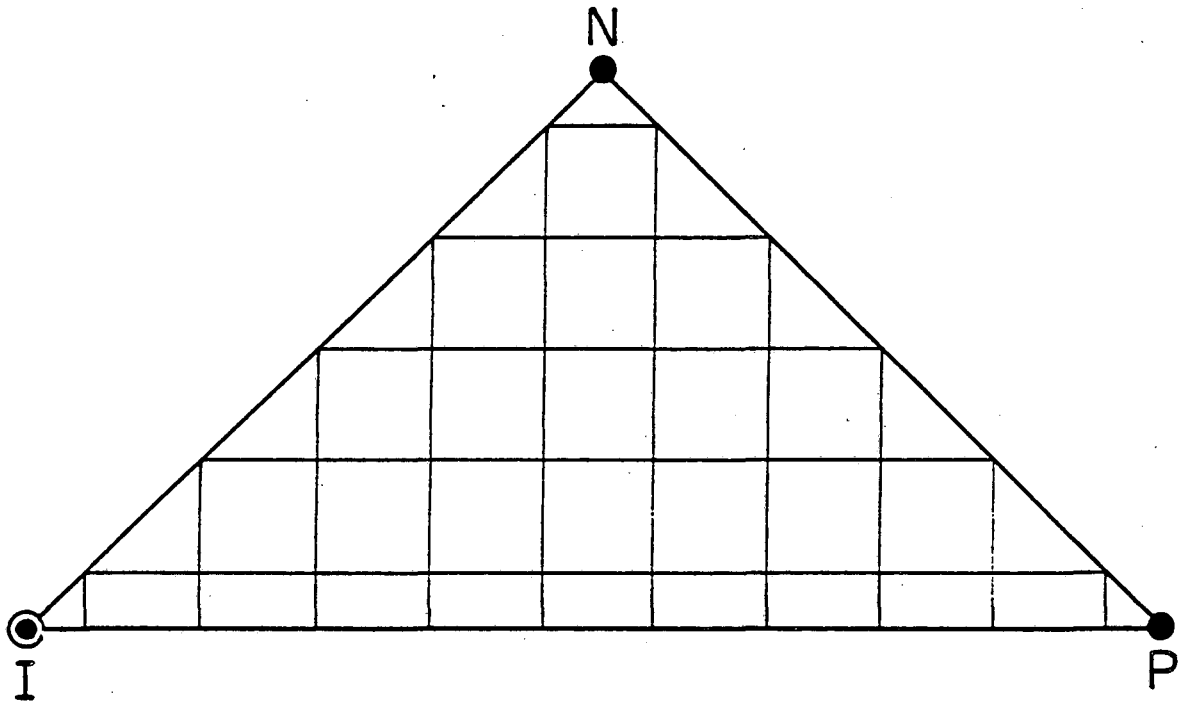

XBL 837-2135

Figure 2. Computational grid five-spot production injection problem (I - injector, P - producer).

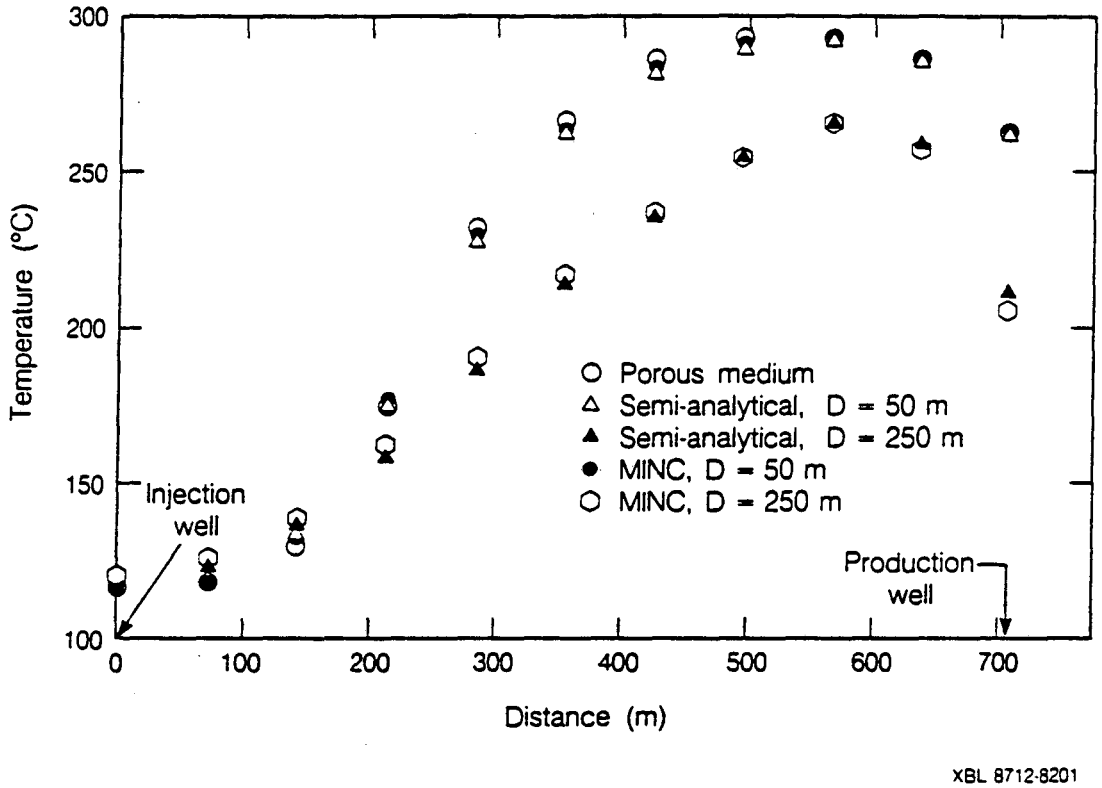

Figure 3. Temperature profiles in the fractures of a five-spot along a line connecting production and injection wells after 36.5 years of production and injection.

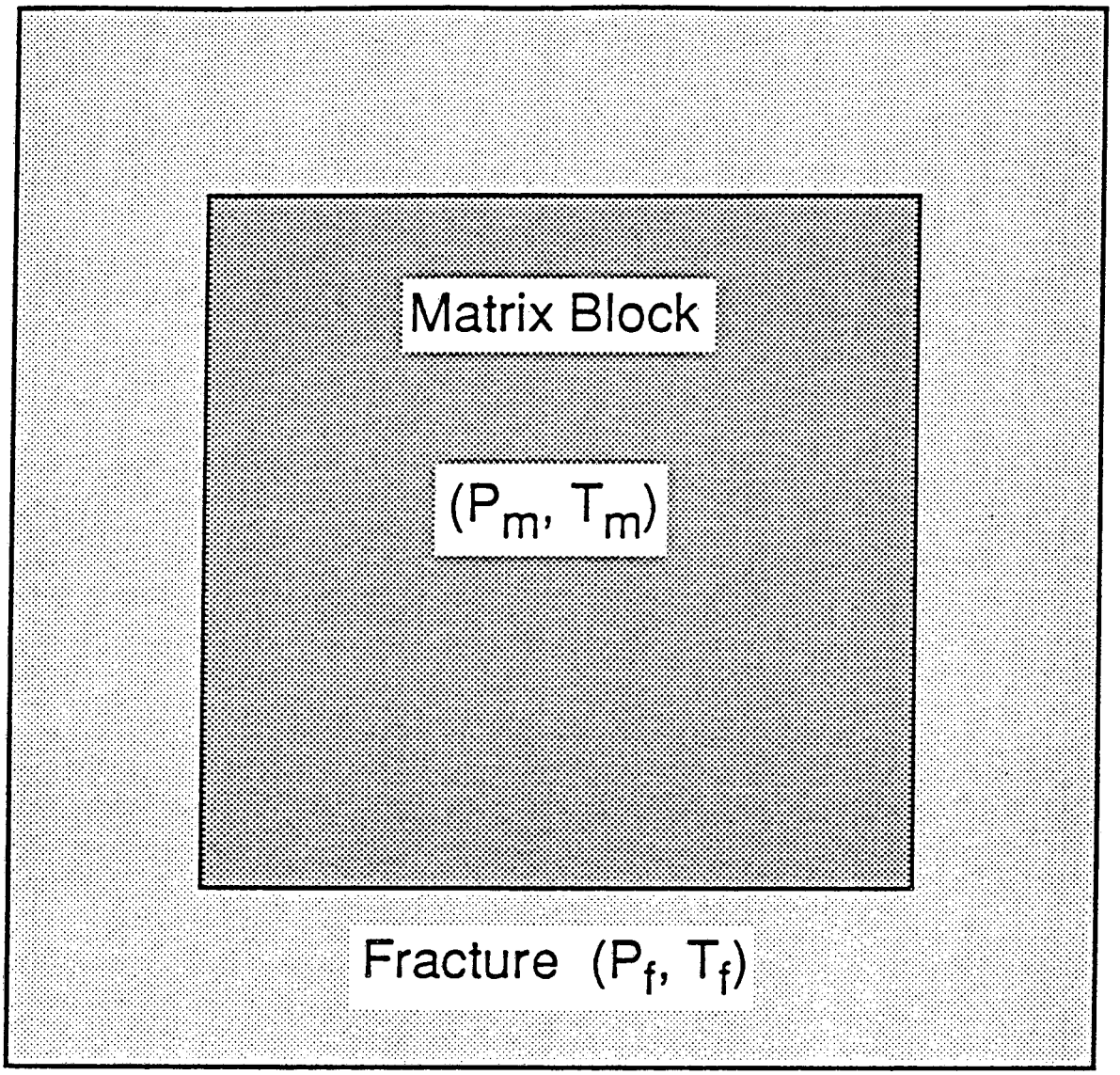

XBL 889-10445

Figure 4. Schematic of single-block problem for evaluating accuracy of semi-analytical fluid and heat exchange.

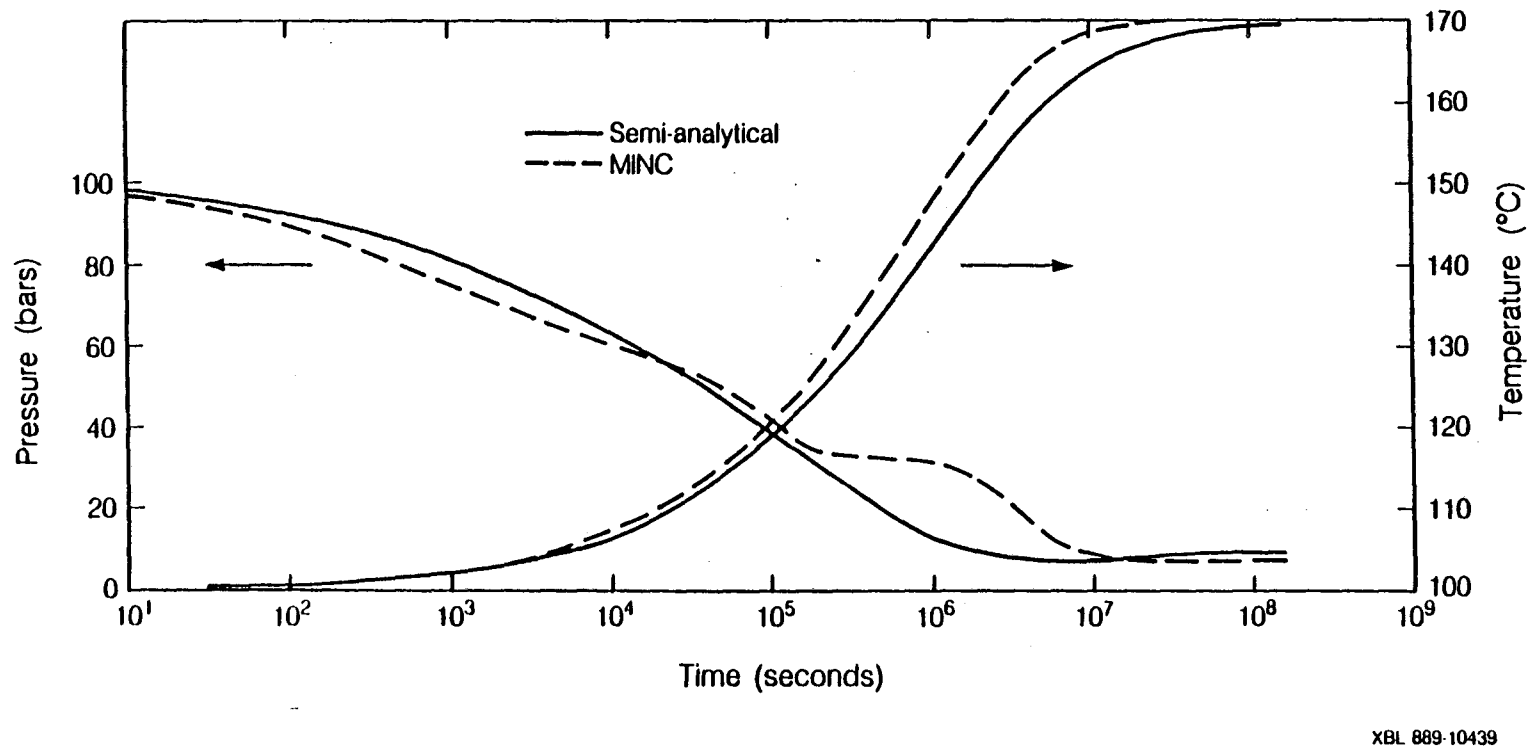

Figure 5. Fracture pressures and temperatures in single-block problem (Case 1; see Table 6).

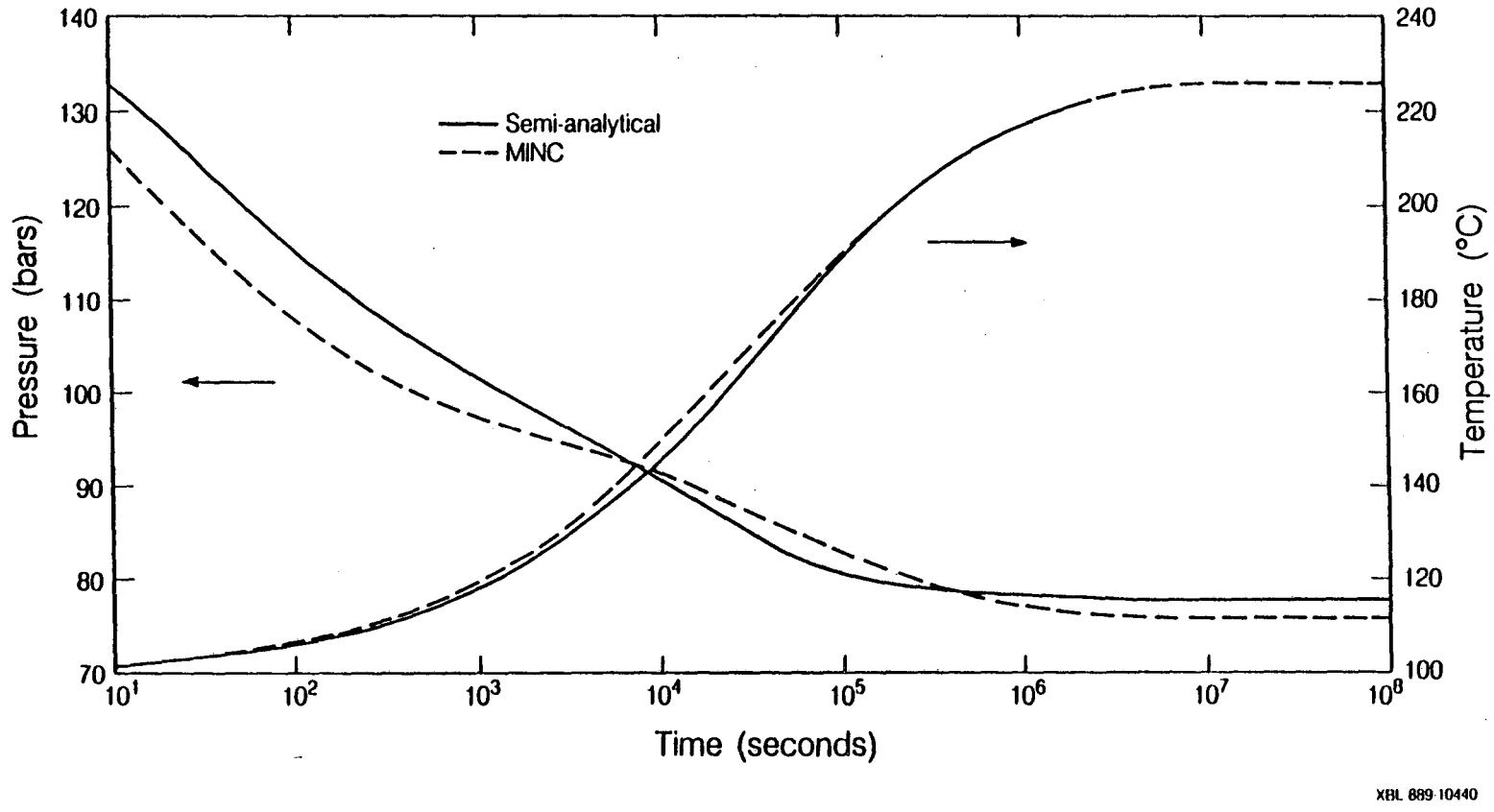

Figure 6. Fracture pressures and temperatures in single-block problem (Case 2; see Table 6).

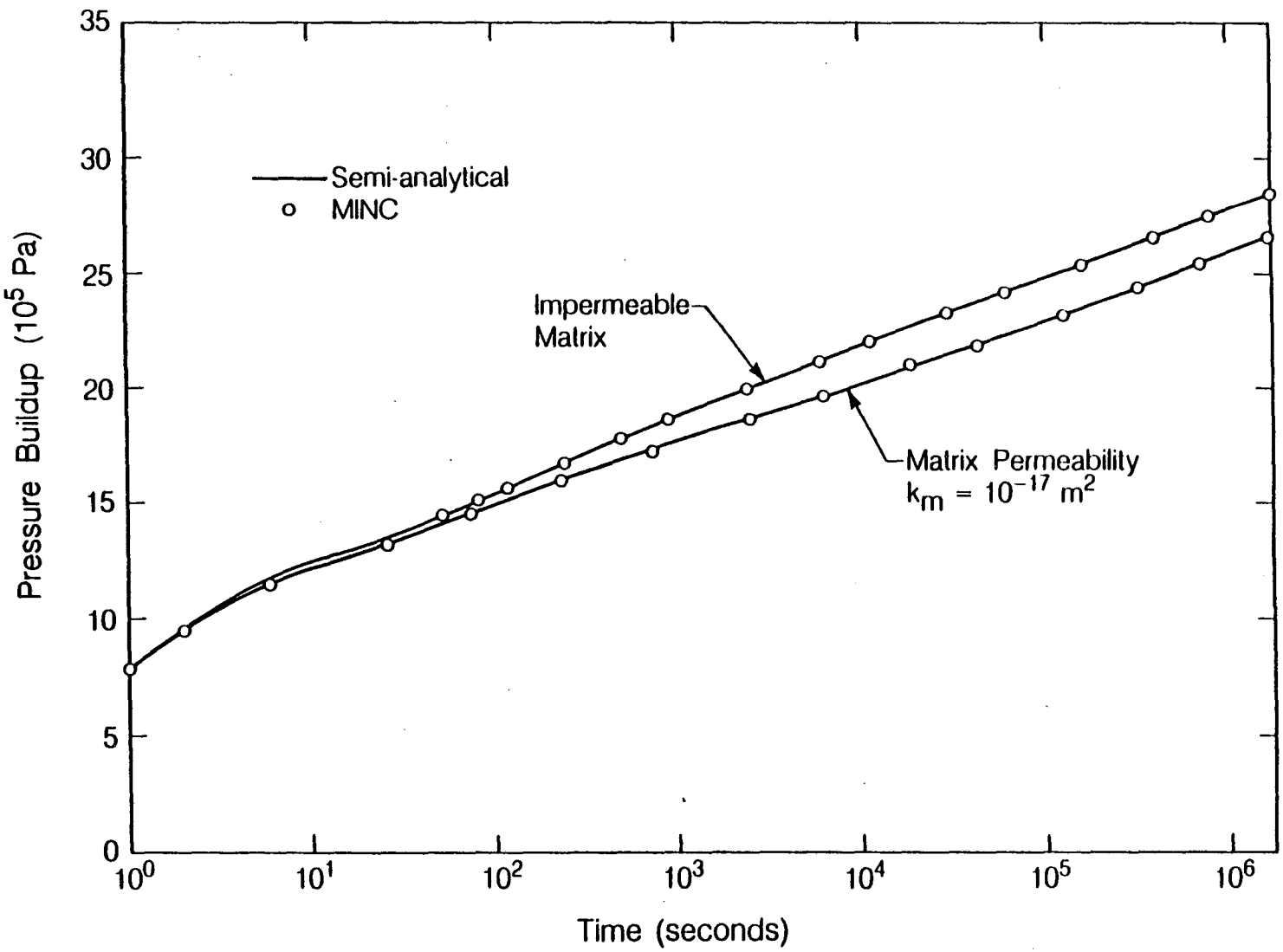

XBL 888-10389

Figure 7. Simulated pressure buildups for non-isothermal injection into a fractured reservoir ($10 \times 10 \times 10$ m^3 cubic matrix blocks)

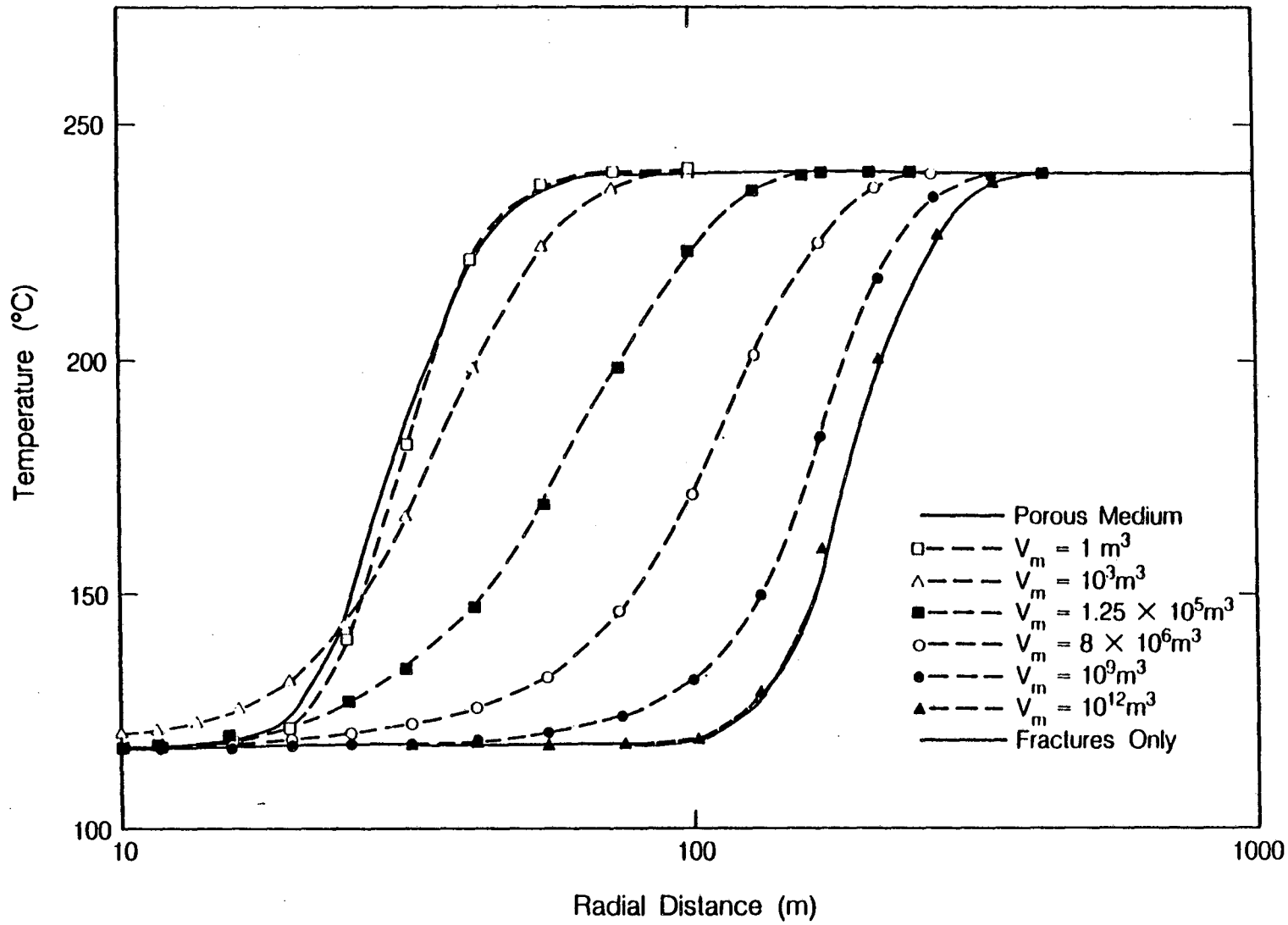

XBL 889-10442

Figure 8. Temperature profiles in the fractures after 49.3 days of injection.

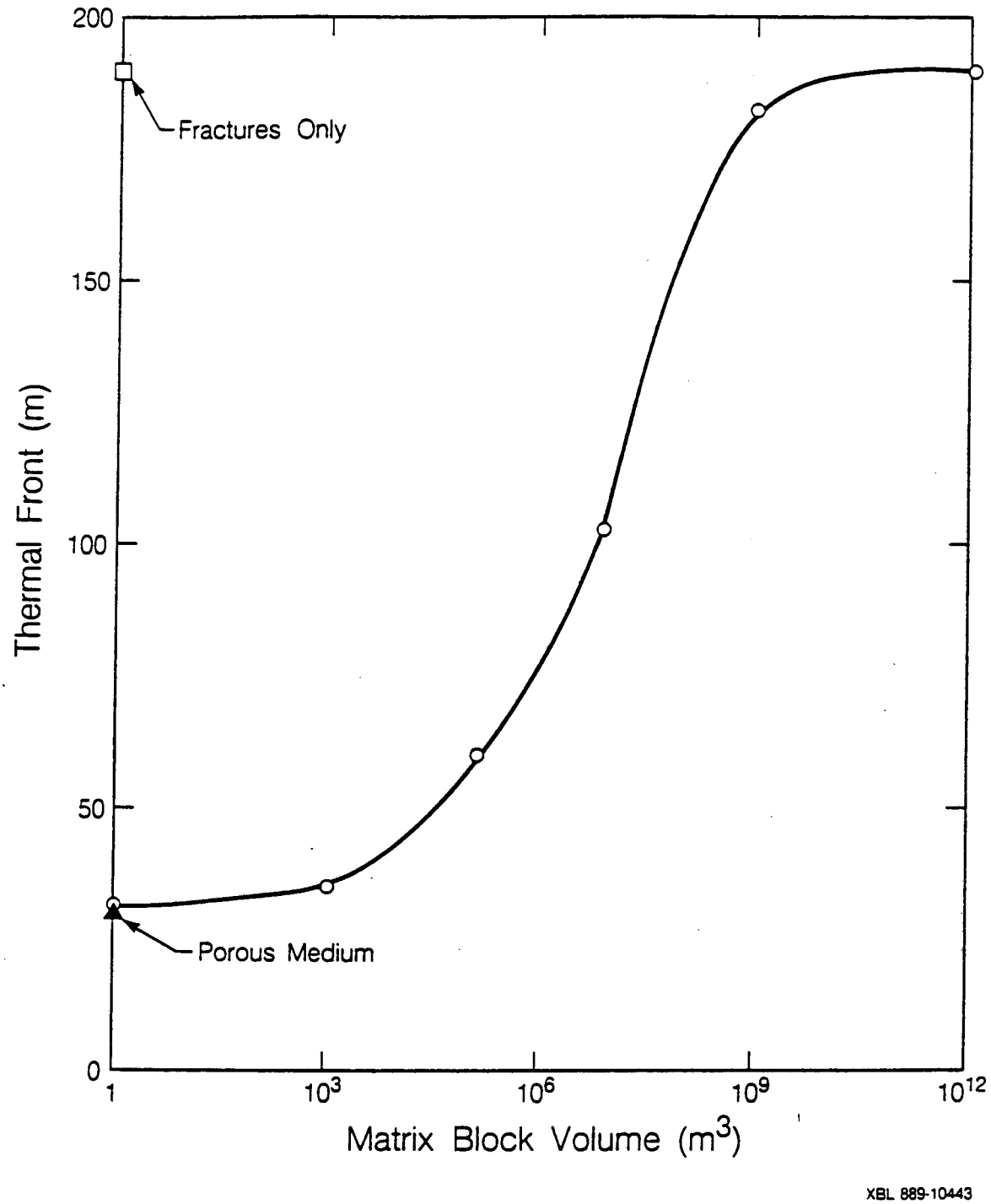

Figure 9. Location of thermal front after 49.3 days of injection as function of matrix block size.

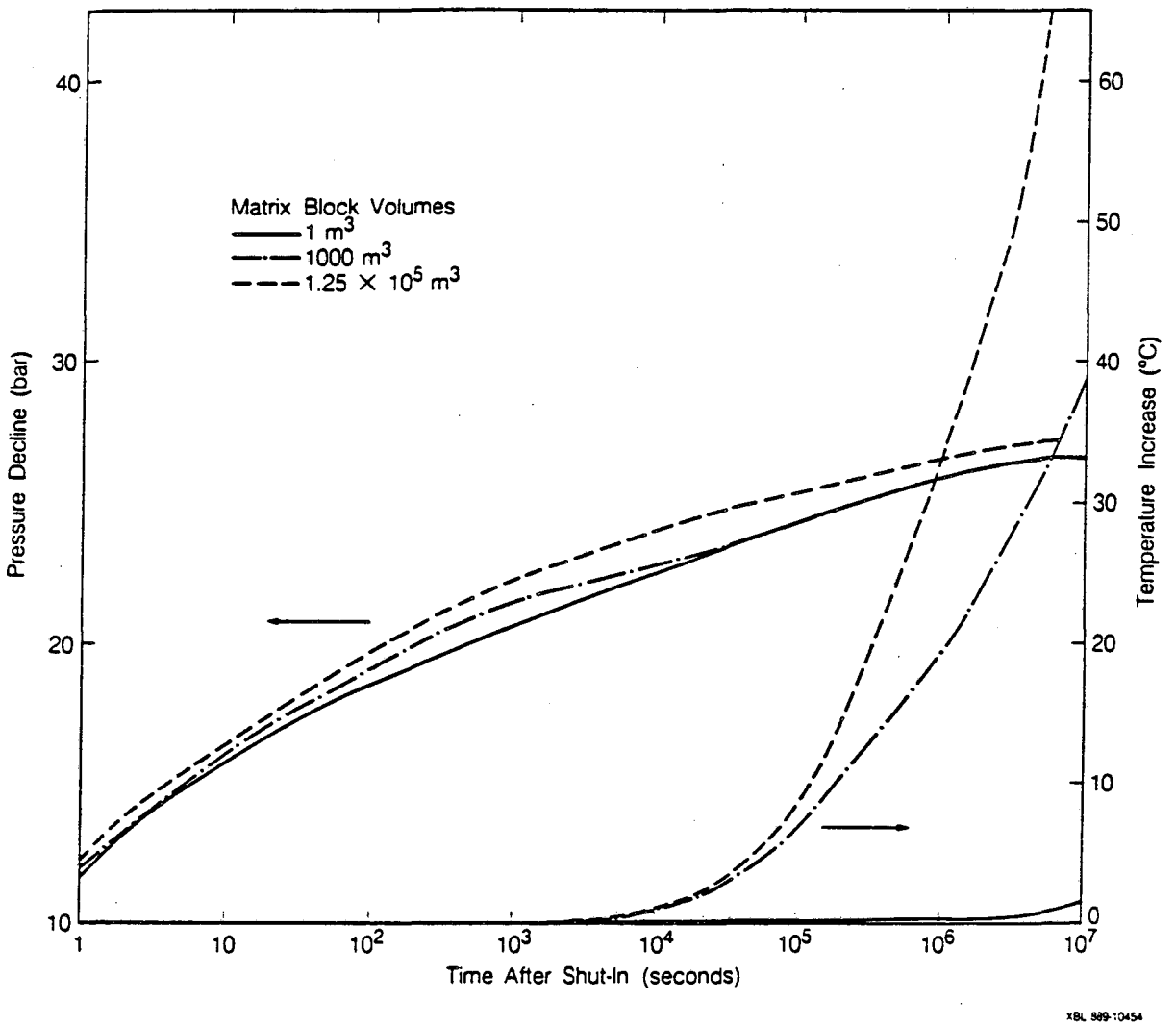

Figure 10. Temperature and pressure transients following shut-in of injection well after 11.6 days.

LAWRENCE BERKELEY LABORATORY
TECHNICAL INFORMATION DEPARTMENT
UNIVERSITY OF CALIFORNIA
BERKELEY, CALIFORNIA 94720